$H + CH_2CO \rightarrow CH_3 + CO$ AT HIGH TEMPERATURE : A HIGH PRESSURE CHEMICAL ACTIVATION REACTION WITH POSITIVE BARRIER

by

J. Hranisavljevic, S. S. Kumaran,[#] and J. V. Michael*
Chemistry Division, Argonne National Laboratory, Argonne, IL 60439, USA

Corresponding Author: **Dr. J. V. Michael**
D-193, Bldg. 200
Argonne National Laboratory
Argonne, IL 60439, USA
Phone: (630) 252-3171, Fax: (630) 252-4470
E-mail: Michael@anlchm.chm.anl.gov

(27th Symp. (Int'l) on Combust., November, 1997)

Presentation Mode: Oral Presentation
Preferred Publication: Proceedings
Category: Reaction Kinetics

	Text	Reference	Tables	Figures	Total
Count	9 pages	23 citations	2 pages	5 pages	
Equiv. Words	2873	383	800	1000	5056

[#]Present address: Cabot Corporation, 700 E. US Highway 36, Tuscola, IL 61953.

This work was supported by the U. S. Department of Energy, Office of Basic Energy Sciences, Division of Chemical Sciences, under Contract No. W-31-109-Eng-38.

DISCLAIMER

DISCLAIMER

Portions of this document may be illegible in electronic image products. Images are produced from the best available original document.

Abstract

The Laser Photolysis-Shock Tube (LP-ST) technique coupled with H-atom atomic resonance absorption spectrometry (ARAS) has been used to study reaction, $H + CH_2CO \rightarrow CH_3 + CO$, over the temperature range, 863–1400 K. The results can be represented by the Arrhenius expression, $k = (4.85 \pm 0.70) \times 10^{-11} \exp(-2328 \pm 155\ K/T)\ cm^3\ molecule^{-1}\ s^{-1}$. The present data have been combined with the earlier low temperature flash photolysis-resonance fluorescence measurements to yield a joint three parameter expression, $k = 5.44 \times 10^{-14}\ T^{0.8513} \exp(-1429\ K/T)\ cm^3\ molecule^{-1}\ s^{-1}$. This is a chemical activation process that proceeds through vibrationally excited acetyl radicals. However, due to the presence of a low lying forward dissociation channel to $CH_3 + CO$, the present results refer to the high pressure limiting rate constants. Hence, transition state theory with Eckart tunneling is used to explain the data.

stabilization simply cannot compete with forward dissociation using any RRK (or RRKM) model.

In an RRK (or RRKM) formulation, the rate constant based on H-atom depletion for reaction (1), through CH_3CO^*, can be expressed as:

$$k_H = k_{add} \int_{\varepsilon_o}^{\infty} \frac{(k_{f\varepsilon} + \beta\omega)\, f(\varepsilon)d\varepsilon}{(k_{f\varepsilon} + k_{b\varepsilon} + \beta\omega)}, \qquad (2)$$

where k_{add}, $k_{f\varepsilon}$, $k_{b\varepsilon}$, β, ω, and $f(\varepsilon)$ refer to (a) the high pressure rate constant for reaction (1), (b) the specific RRK (or RRKM) rate constant for forward dissociation from CH_3CO^*, (c) the specific RRK (or RRKM) rate constant for backward dissociation to give reactants at the threshold energy, ε_o, (d) the collisional deactivation efficiency, (e) the collision rate constant, and (f) the RRK (or RRKM) normalized distribution function for a given temperature, respectively. In view of the above discussion, $k_{f\varepsilon} >> (k_{b\varepsilon} + \omega\beta)$ in which case $k_H = k_{add}$; i. e., the high pressure limiting rate constant. This is why Michael et al. [6] suggested that reaction (1) should be compared to 0.5 of the high pressure limit for $H + C_2H_4$ which was directly measured by Lee et al. [7].

There are four direct studies at low temperature [3,4,6,8] three of which have already been discussed by Michael et al. [6] who report $k_1 = (1.88 \pm 0.12) \times 10^{-11}$ $\exp(-1725 \pm 190\ K/T)$ cm^3 $molecule^{-1}$ s^{-1} for $298 \leq T \leq 500$ K. The Unemoto et al. results [8], expressed as $k_1 = 6.47 \times 10^{-12} \exp(-947\ K/T)$ cm^3 $molecule^{-1}$ s^{-1} for $240 \leq T \leq 440$ K, disagree with Michael et al. by about a factor of two to four. This disagreement can probably be traced to secondary reaction perturbations in the pulse radiolysis-resonance absorption experiments [8] since such perturbations are possible and were noted in the earlier work [6]. The high temperature shock wave results of Frank et al. give $k_1 = 2.99 \times 10^{-11}$ cm^3 $molecules^{-1}$ s^{-1} for $1650 \leq T \leq 1850$ K [9]. These results were derived from mechanistic fits of CH_2CO decomposition experiments. In a second shock wave study,

Hidaka et al. [10] report an expression (k_1 = 1.84 x 10^{-17} $T^{2.0}$ exp(-1007 K/T) cm^3 $molecules^{-1}$ s^{-1}) that was consistent with their own data, that of Michael et al., and that of Frank et al. They subsequently used this result to understand the oxidation of CH_2CO [11].

Experimental

The present experiments were performed with the laser photolysis-shock tube (LP-ST) technique, and the method and the apparatus currently being used have been previously described [12,13]. Therefore, only a brief description of the experiment will be presented here.

The apparatus consists of a 7-m (4-in. o.d.) 304 stainless steel tube separated from the He driver chamber by a 4-mil unscored 1100-H18 aluminum diaphragm. The tube was routinely pumped between experiments to $<10^{-8}$ Torr by an Edwards Vacuum Products Model CR100P packaged pumping system. The velocity of the shock wave was measured with eight equally spaced pressure transducers (PCB Piezotronics, Inc., Model 113A2) mounted along the end portion of the shock tube, and temperature and density in the reflected shock wave regime were calculated from this velocity and include corrections for boundary layer perturbations [14-16]. Both the 4094C Nicolet digital oscilloscope and the Questek 2000 excimer laser were triggered by delayed pulses that derive from the last velocity gauge signal.

The 193.3 nm radiation was produced by a Questek 2000 excimer laser operated in the ArF mode. The beam was directed by two reflectors, and entered the shock tube through a suprasil grade quartz window that was mounted flush to the endplate. The H-atom atomic resonance absorption spectrometric (ARAS) detection was used to follow $[H]_t$, as described previously [17]. The photometer system was radially located at the distance of 6 cm from the endplate. MgF_2 components were used in the photometer optics. The resonance lamp beam was detected by an EMR G14 solar blind photomultiplier tube. The laser beam was attenuated by screens so that $[H]_0 \leq \sim 1x10^{12}$

atoms cm^{-3}. At this concentration level, secondary reactions with other species are negligible over the observation time. In the present studies, sufficient [H] was produced from the photolysis of the reactant, CH_2CO [18]. Since ARAS detection is sensitive, insignificant amounts of CH_2CO were destroyed, and therefore $[CH_2CO]_0$, calculated from initial mixing ratios and thermodynamic conditions in reflected shock waves, was taken to be constant.

For the range of [H] used in these experiments, Beer's law is valid, and, therefore, $[H]_t = (ABS)_t / \sigma\ell$ where $(ABS)_t \equiv -\ell n(I_t / I_0)$ (I_t and I_o refer to time-dependent and incident photometric intensities, respectively, σ is the effective atom cross section, and ℓ is the absorption path length). Hence, the pseudo-first-order H-atom depletion due to reaction (1) follows the equation:

$$\ell n(ABS)_t = -k_{1st}t + \text{Const.} \qquad (3)$$

The data was analyzed according to eqn. (3) using linear-least squares methods. A typical result is shown in Fig. 1. For each experiment, the derived values for k_{1st} are reported in Table 1. Since $[CH_2CO]$ is effectively constant, the second-order rate constant is given by $k_1 = k_{1st} / [CH_2CO]_0$, and these are likewise listed in Table 1.

Gases. Kr diluent for the experimental mixtures was obtained from MG Industries (Scientific Grade, 99.996%) and was used without further purification. He, used as the driver gas and also in the resonance lamp and atomic filter section, was Ultra-High Purity Grade (99.995%) and was obtained from Airco Industrial Gases. In the atomic filter section, H_2 from Airco Industrial Gases (Pre-Purified, 99.995%) was used as received. CH_2CO was prepared from the pyrolysis of diketene [19] and was further purified by bulb-to-bulb distillation in a greaseless, all-glass, high-vacuum gas handling system. The middle third was retained. Mass spectral analysis showed that the sample was >96%, the principal impurity being allene.

Results

The bimolecular rate constant results, k_1, from Table 1 are plotted in Arrhenius form in Fig. 2. Over the temperature range, 863-1400 K, the results can be represented by:

$$k_1 = (4.85 \pm 0.70) \times 10^{-11} \exp(-2328 \pm 155\ K/T)\ cm^3\ molecule^{-1}\ s^{-1}, \qquad (4)$$

using linear least squares analysis. The straight line shown in the figure is calculated from eqn. (4). If this equation is extrapolated to the temperature range of the Frank et al. experiments [9], the value determined at 1750 K is 1.28×10^{-11} in contrast to their value of 2.99×10^{-11} cm^3 $molecule^{-1}$ s^{-1}. The expression, determined by Michael et al., extrapolated from 200–500 K up to the mean temperature of the present study, gives $k_1(1100\ K) = 3.92 \times 10^{-12}$ whereas eqn. (4) gives 5.84×10^{-12} cm^3 $molecule^{-1}$ s^{-1}. This behavior is consistent with slight T-dependence in the A-factor, and this possibility was recognized by Hidaka et al. [10] whose expression agreed with both Michael et al. and Frank et al., namely $k_1 = 1.84 \times 10^{-17}\ T^{2.0} \exp(-1007\ K/T)\ cm^3\ molecule^{-1}\ s^{-1}$. This latter expression predicts $k_1(1100\ K) = 8.91 \times 10^{-12}$ cm^3 $molecule^{-1}$ s^{-1}, a value that is higher than the present by ~50%.

Discussion

Figure 3 shows a composite plot of the present results and those of Michael et al. [6]. The two combined data sets can be fitted to a three parameter expression by least squares analysis yielding:

$$k_1 = 5.44 \times 10^{-14}\ T^{0.8513} \exp(-1429\ K/T)\ cm^3\ molecule^{-1}\ s^{-1}, \qquad (5)$$

over the 298–1400 K range. Eqn. (5) predicts values within ±4% of the linear least squares Arrhenius expressions that represent the present and earlier [6] results. The line drawn in Fig. 3 is calculated from eqn. (5).

As discussed in the Introduction, k_1 refers to the high pressure limiting rate constant for H addition to CH_2CO. Hence, theoretical values for the rate constant can be calculated using transition state theory (TST) if both the force fields and energetics of the transition state are known. Such information is already available from Osborn et al. (labeled TS2 in Table IV of [5]), and these results are included here in Table 2. We have calculated conventional TST rate constants from:

$$k = \Gamma (k_b T/h) (Q^{\ddagger}/Q_H Q_{CH_2CO}) \exp(-E_0/k_b T), \quad (6)$$

using their result without adjustments over the temperature range, 300–1400 K. Γ is the Eckart (E) tunneling factor, k_b is Boltzmann's constant, T is temperature, the Q's are partition functions, and E_0 is the zero point corrected electronic energy barrier for the transition state relative to $H + CH_2CO$.

The calculation is shown in Fig. 4 in comparison to the experimental result represented by eqn. (5) in Fig. 3. Clearly, this transition state does not give good predictions for the rate behavior at the TST/E level of calculation. The zero point energy corrected barrier height is 5.535 kcal mole^{-1}. Generally, G2Q: QCISD/6–311G** level electronic structure calculations are accurate to ±1 kcal mole^{-1} for stable molecules, and the Osborn et al. [5] prediction for ΔH^0_{01}, -41.74 kcal mole^{-1}, is in excellent agreement with the experimental value, (-41.9 ± 0.5) kcal mole^{-1} [21]. However, the same level of calculation applied to radicals is less accurate giving values within ~±2 kcal mole^{-1}. Hence, we have adjusted the barrier height within these limits (i. e., to 4.306 kcal mole^{-1}, indicated by the value in parentheses in Table 2) to see if better agreement can be obtained at the TST/E level of calculation. The Osborn et al. transition state still gives disappointing predictions being 20% lower and 60% higher than experiment at 300 and 1400 K, respectively, as shown in Fig. 4. Generally, high values at high temperatures mean that transition states have too many low frequency bends at $\nu \cong$ 300–600 cm^{-1}. If the Osborn et al. transition

state vibration frequencies [5] are examined, there are four such frequencies that are essentially canceled by three in CH_2CO. The one remaining frequency (309 cm^{-1}) predicts too much curvature at high temperature.

We carried out lower level *ab initio* (HF/6–31G*) optimized calculations, as a function of the CH bond length for the incoming atom, and these calculations gave a transition state at a CH bond distance of 1.80 Å with a zero point corrected barrier height of 10.3 kcal $mole^{-1}$, to be contrasted to 1.89 Å and 5.535 kcal $mole^{-1}$, respectively, from Osborn et al. This suggests that the transition state is highly dependent on the level of *ab initio* theory. In any case, it is obvious that energy scaling is necessary in order to explain the experimental results using either the Osborn et al. or the present lower level transition states. Because it is a higher level calculation, we have elected to modify the Osborn et al. transition state in a two parameter fit which minimizes the error between prediction and experiment.

TST/E calculations have been carried out with variations in both the barrier height and the two new low lying bending frequencies (considered to be degenerate). The parametrically varied values are then compared to the experimental results as summarized by eqn. (5). A minimum one standard deviation error of 5.832% between theory and eqn. (5) is reached when the zero point corrected barrier height is 3.907 kcal $mole^{-1}$ and the degenerate bends are 515 cm^{-1}. This successful transition state and its properties are given as ‡(1) in Table 2. The comparison between theory and experiment is shown in Fig. 5. The theoretical results can be expressed to within ±0.1% by the three parameter expression:

$$k_1^{th} = 1.380 \times 10^{-15}\, T^{1.3354} \exp(-1121.4\ K/T)\ cm^3\ molecule^{-1}\ s^{-1}, \qquad (7)$$

over the temperature range, 300-1500 K. At all temperatures, eqn. (7) agrees with the present experimental evaluation, eqn. (5), to within ~±10%. The four low valued vibration

frequencies (500-600 cm^{-1}) in ‡(1) effectively cancel three such values in CH_2CO leaving one value of 515 cm^{-1} in ‡(1). This results in the mild Arrhenius plot curvature of Fig. 5.

In our HF/6–31G* level calculations, we found that the low lying bending vibrations vary rapidly with configuration. With small changes in configuration, it is probable that the same vibrations would also be highly variable, using the Osborn et al. electronic structure methods, had they carried out several additional calculations along the minimum energy path. Therefore, if electronic structure calculations of transition states are not of the highest accuracy then these rapidly varying bending frequencies cannot be highly accurate. This realization partially justifies the present parametric adjusments to the Osborn et al. transition state. From our optimized calculations along the minimum energy path, we also tested whether variational effects might be important; however, we found that the Boltzmann's factors change so rapidly with structure that the only important configuration is the classical transition state; i. e., variational effects are not important. However, this conclusion may not be entirely correct for the higher level Osborn et al. calculations. The present fits are dependent on the choice of dynamical method. Use of a more realistic method for tunneling corrections might alter this conclusion. Also, if Osborn et al. had carried out a sufficient number of transition state calculations along the minimum energy path, then variational effects might be shown to be more important than indicated by the present lower level calculations. As was suggested for the Cl + H_2/D_2 reactions [22], using higher level dynamical theory along with substantially more electronic structure calculations of the type presented by Osborn et al., might eventually give a better explanation of the present data. When such *ab initio* calculations are unavailable, the scaling of both energy [12,13] and, when necessary, vibration frequencies, is still a good theoretical strategy. Even though this is a parametric procedure, the conclusions from lower level efforts still serve to define and delineate the theoretical issues.

Acknowledgments: The authors thank Dr. L. B. Harding for valuable discussions. This work was supported by the U. S. Department of Energy, Office of Basic Energy Sciences, Division of Chemical Sciences, under Contract No. W-31-109-Eng-38.

References

[1] Turner, B. E., *Astrophys. J.* 213:L75 (1977)

[2] Warnatz J., in *Combustion Chemistry* (Ed. W. C. Gardiner, Jr.), Springer-Verlag, New York, 1984, p. 197.

[3] Carr, Jr., R. W., Gay, I. D., Glass, G. P. and Niki, H., *J. Chem. Phys.* 49:846-852 (1968)

[4] Slemr, F. and Warneck, P., *Ber. Bunsenges. Phys. Chem.* 79:152-156 (1975)

[5] Osborn, D. L., Choi, H., Mordaunt, D. H., Bise, R. T., Neumark, D. M. and Rohlfing, C. M., *J. Chem. Phys.* 106:3049-3066 (1997)

[6] Michael, J. V., Nava, D. F., Payne, W. A. and Stief, L. J., *J. Chem. Phys.* 70:5222-5227 (1979)

[7] Lee, J. H., Michael, J. V., Payne, W. A. and Stief, L. J., *J. Chem. Phys.* 68:1817-1820 (1978)

[8] Unemoto, H., Tsunashima, S., Sato, S., Washida, N. and Hatakeyama, S., *Bull. Chem. Soc. Jpn.* 57:2578-2580 (1984)

[9] Frank, P., Bhaskaran, K. A. and Just, Th., *J. Phys. Chem.* 90:2226-2231 (1986)

[10] Hidaka, Y., Kimura, K. and Kawano, H., *Comb. Flame* 99:18-28 (1994)

[11] Hidaka, Y., Kimura, K., Hattori, K. and Okuno, T., *Comb. Flame* 106:155-167 (1996)

[12] Michael, J. V., *Prog. Energy Combust. Sci.* 18:327-347 (1992)

[13] Michael, J. V., in *Advances in Chemical Kinetics and Dynamics* (Ed. J. R. Barker), JAI, Greenwich, 1992, Vol. I, pp. 47-112, for original references.

[14] Michael, J. V. and Sutherland, J. W., *Int. J. Chem. Kinet.* 18:409-436 (1986)

[15] Michael, J. V., *J. Chem. Phys.* 90:189-198 (1989)

[16] Michael, J. V. and Fisher J. R., in *Seventeenth International Symposium on Shock Waves and Shock Tubes* (Ed. Y. W. Kim) AIP Conference Proceedings 208, American Institute of Physics, New York, 1990, pp. 210-215.

[17] Lim, K. P. and Michael, J. V., *Twenty-Fifth Symposium (International) on Combustion,* The Combustion Institute, Pittsburgh, PA, 1994, pp. 713-719, and references therein.

[18] Glass, G. P., Kumaran, S. S. and Michael, J. V., private communication.

[19] Andreades, S. and Carlson, H. D., *Org. Syn.* Coll. V:679-684 (1973)

[20] Herzberg, G., *Molecular Spectra and Molecular Structure*, D. Van Nostrand, Princeton, 1966, p. 622.

[21] Ruscic, B., private communication, October, 1997.

[22] Kumaran, S. S. and Michael, J. V., *J. Phys. Chem.* 100:20172 (1997)

Table 1: Rate Data for H + CH_2CO by the LP-ST Technique.

P_1 / Torr	[a]M_s	[b]ρ_5 / (10^{18} cm^{-3})	[b]T_5 / K	k_{1st} / s^{-1}	[c]k / (10^{-12} cm^3 s^{-1})
		$X_{CH_2CO} = 5.141 \times 10^{-4}$			
10.66	2.195	1.776	1235	6864	7.52
5.89	2.149	0.956	1188	3924	7.98
5.94	2.143	0.965	1179	3224	6.50
5.98	2.058	0.919	1100	2579	5.46
5.93	2.187	0.984	1226	3479	6.87
5.93	2.341	1.063	1387	5013	9.17
5.92	2.424	1.102	1478	5082	8.97
		$X_{CH_2CO} = 1.332 \times 10^{-4}$			
10.91	1.960	1.574	1006	995	4.75
10.85	2.107	1.723	1145	1447	6.30
10.82	2.288	1.889	1332	2010	7.99
10.86	2.357	1.966	1401	2196	8.38
10.82	2.219	1.830	1256	2163	8.87
10.85	2.036	1.649	1077	1193	5.43
30.84	1.800	3.869	863	1649	3.20
15.79	1.943	2.248	995	1399	4.60
15.97	1.838	2.124	911	1149	4.04
15.97	1.797	2.061	873	756	2.75
		$X_{CH_2CO} = 6.485 \times 10^{-5}$			
16.00	1.975	2.349	1030	811	5.32
15.93	2.032	2.426	1083	886	5.63
15.84	2.095	2.506	1142	905	5.57
15.85	1.870	2.168	935	604	4.29
15.98	2.140	2.602	1182	1427	8.46
15.94	1.911	2.247	970	700	4.80

[a]The error in measuring the Mach number, M_S, is typically 0.5-1.0 % at the one standard deviation level. [b]Quantities with the subscript 5 refer to the thermodynamic state of the gas in the reflected shock region. [c]The rate constants are derived as described in the text.

Table 2: Molecular parameters used for TST/E calculations

Species	CH_2=C=O[a]	TS2 from ref. 5	‡(1)	CH_3C=O from ref. 5
Geometry[b]	$r(C_aC_b)$ = 1.315 $r(C_aO)$ = 1.16 $r(C_bH_c)$ = 1.079 $r(C_bH_b)$ = 1.079 $<(H_cCH_b)$ = 122.3	$r(C_aC_b)$ = 1.340 $r(C_aO)$ = 1.163 $r(C_aH_c)$ = 1.083 $r(C_aH_b)$ = 1.083 $r(C_aH_a)$ = 1.888 $<(C_bC_aO)$ = 172.1 $<(H_cC_bC_a)$ = 116.7 $<(H_bC_bC_a)$ = 116.7 $<(H_aC_bC_a)$ = 111.3 $<(H_cC_bC_aO)$ = 105.0 $<(H_bC_bC_aO)$ = -105.0 $<(H_aC_bC_aO)$ = 0.0	$r(C_aC_b)$ = 1.340 $r(C_aO)$ = 1.163 $r(C_aH_c)$ = 1.083 $r(C_aH_b)$ = 1.083 $r(C_aH_a)$ = 1.888 $<(C_bC_aO)$ = 172.1 $<(H_cC_bC_a)$ = 116.7 $<(H_bC_bC_a)$ = 116.7 $<(H_aC_bC_a)$ = 111.3 $<(H_cC_bC_aO)$ = 105.0 $<(H_bC_bC_aO)$ = -105.0 $<(H_aC_bC_aO)$ = 0.	$r(C_aC_b)$ = 1.513 $r(C_aO)$ = 1.196 $r(C_aH_c)$ = 1.092 $r(C_aH_b)$ = 1.092 $r(C_aH_a)$ = 1.093 $<(C_bC_aO)$ = 127.5 $<(H_cC_bC_a)$ = 108.6 $<(H_bC_bC_a)$ = 108.6 $<(H_aC_bC_a)$ = 111.1 $<(H_cC_bC_aO)$ = 121.6 $<(H_bC_bC_aO)$ = -121.6 $<(H_aC_bC_aO)$ = 0.0
Energy (kcal mole^{-1})	41.739[c,d]	47.274[d] (46.045)[e]	(45.646)[e]	0
Frequencies (cm^{-1})	433, 528, 588, 977, 1118, 1388, 2152, 3070, 3166	309, 426, 567, 571, 799, 1033, 1118, 1425, 2194, 3202, 3304, 801*i*	515, 515, 567, 571, 799, 1033, 1118, 1425, 2194, 3202, 3304, 801*i*	85, 454, 827 938, 1037, 1356 1432, 1433, 1913, 2871, 2946, 2950
Moments of inertia (g cm^2)	2.98 x 10^{-40} 8.15 x 10^{-39} 8.46 x 10^{-39}	8.42 x 10^{-40} 9.16 x 10^{-39} 9.42 x 10^{-39}	8.42 x 10^{-40} 9.16 x 10^{-39} 9.42 x 10^{-39}	9.66 x 10^{-40} 8.38 x 10^{-39} 8.84 x 10^{-39}

[a] Bond distances, angles, vibrational frequences, and moments of inertia from ref. 20.
[b] The following atom labels have been used: C_a is connected to O; C_b is the end carbon in both CH_2=C=O and CH_3C=O; H_a is attacking H atom; and H_b and H_c are initially part of CH_2=C=O.
[c] Energy of H + CH_2=C=O.
[d] Energies from ref. 5, expressed relative to CH_3C=O.
[e] Fitted to agree with experimental data.

Figure Captions

Fig. 1 First-order decay plot, $\ell n(ABS)_t$ against time, according to eqn.. (3). $k_{1st} = (2163 \pm 87)\ s^{-1}$ for an experiment at $P_1 = 10.82$ Torr and $M_s = 2.219$. $T_5 = 1256$ K and $[CH_2C{=}O] = 2.438 \times 10^{14}\ cm^{-3}$. The corresponding second-order rate constant is 8.87×10^{-12} $cm^3\ molecule^{-1}\ s^{-1}$.

Fig. 2 Arrhenius plot of the data from Table1. The line is given by eqn.. (4) and the solid circles are the individual data points.

Fig. 3 Composite plot of the present data and low temperature data from ref. [6] fitted to a 3-parameter expression given by eqn. (5).

Fig. 4 Comparison of the experimental results, eqn. (5), (——), to TST/E predictions using the TS2 structure from ref. 5 without energy barrier adjustment (.....) and with the energy barrier fitted to the experimental data at 600 K (------).

Fig. 5 Comparison of the experimental results (●) to TST/E prediction for the ‡(1) structure of Table 2 (——).

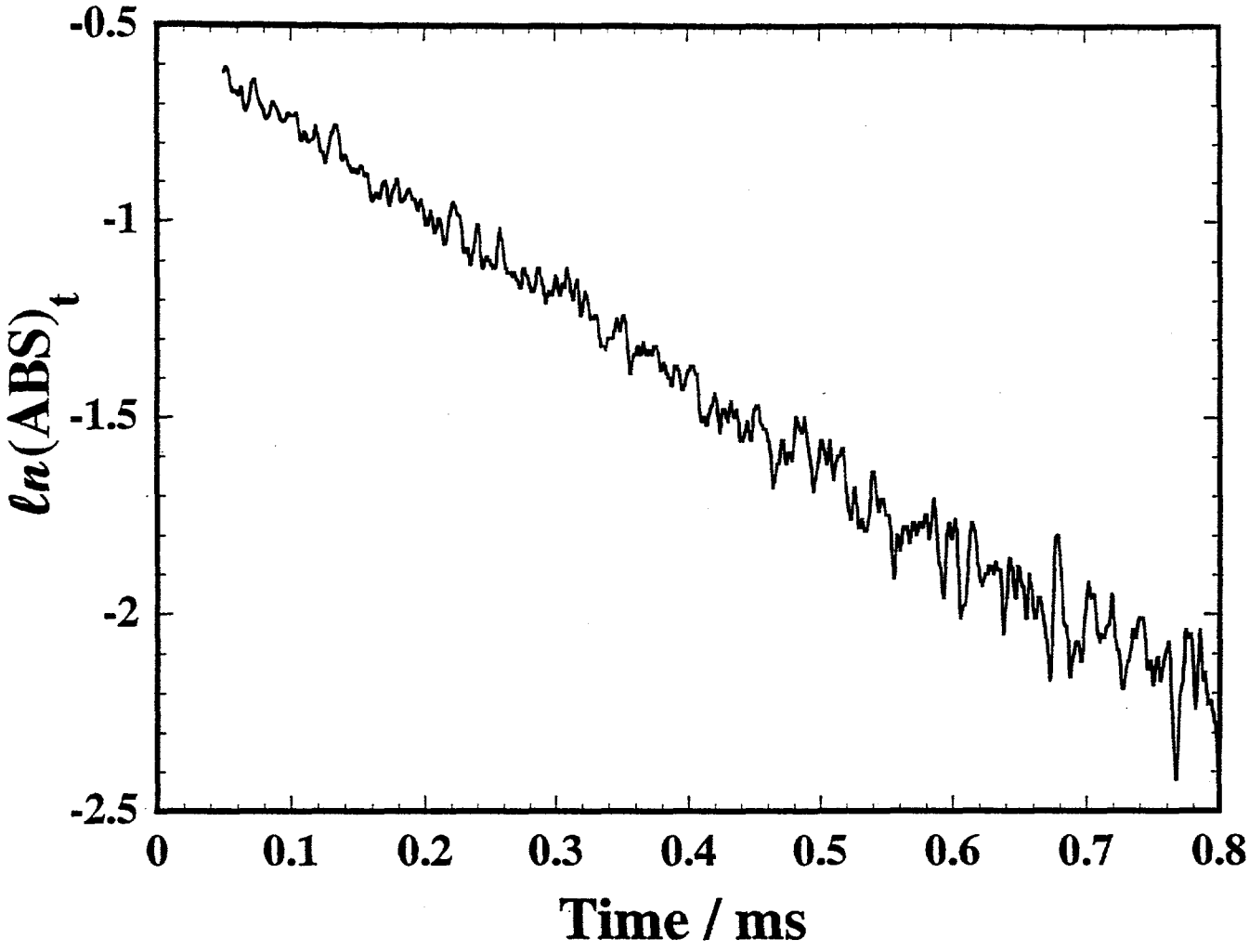

FIGURE 1

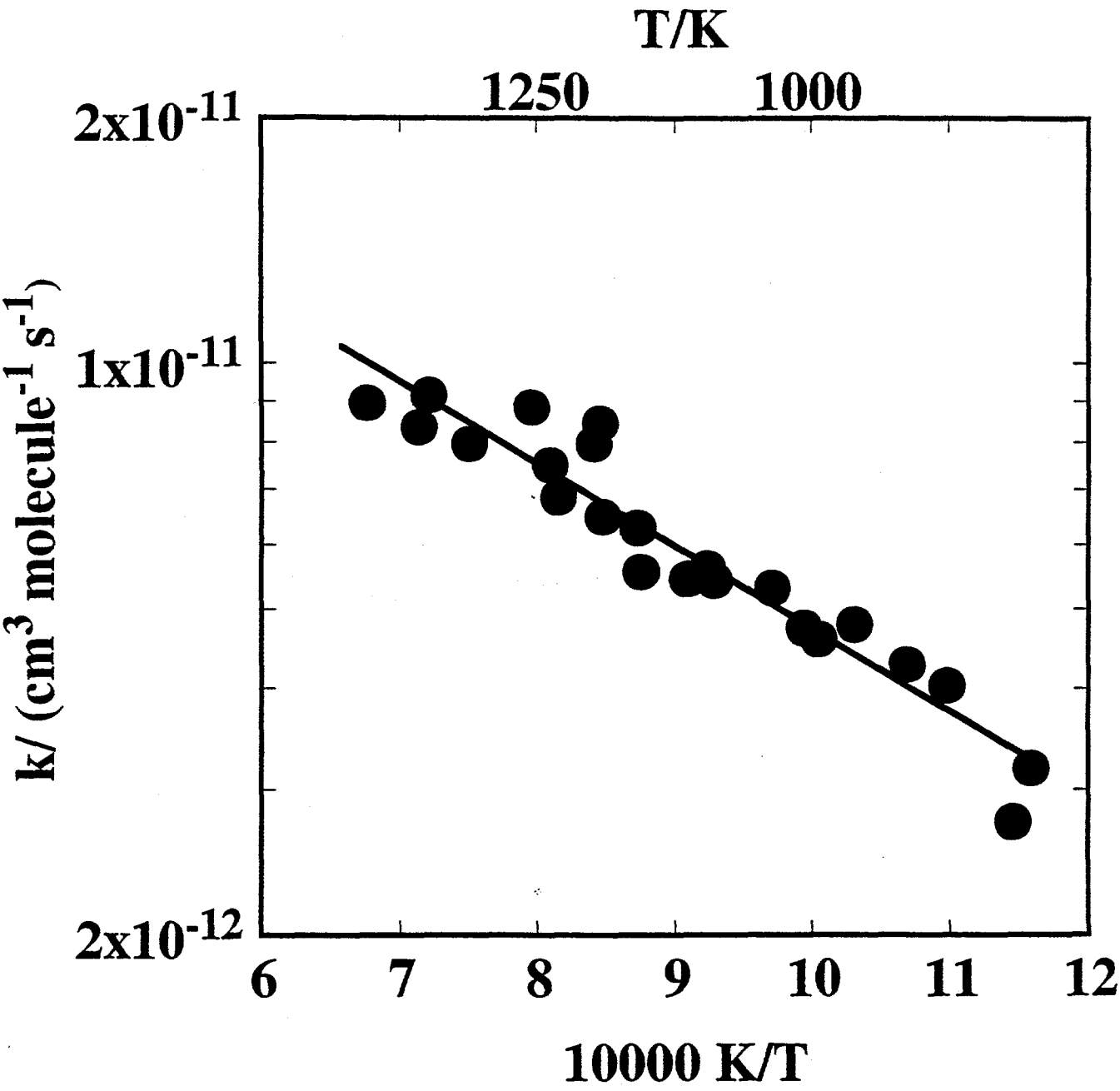
T/K
1250
1000
2x10-11
1x10-11
2x10-12
k/ (cm3 molecule-1 s-1)
6
7
8
9
10
11
12
10000 K/T

FIGURE 2

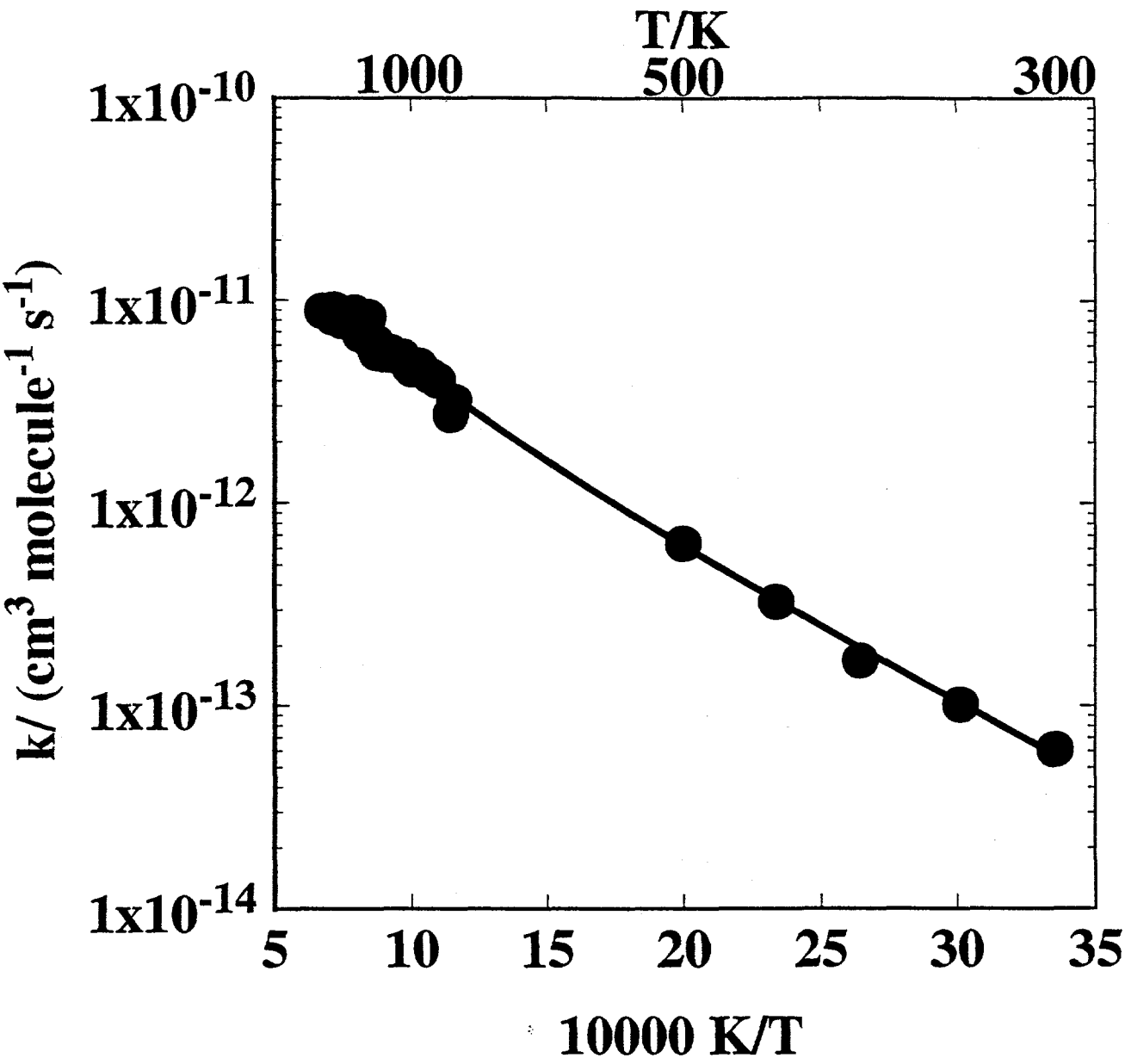
T/K
1000
500
300
1x10-10
1x10-11
1x10-12
1x10-13
1x10-14
k/ (cm3 molecule-1 s-1)
5
10
15
20
25
30
35
10000 K/T

FIGURE 3

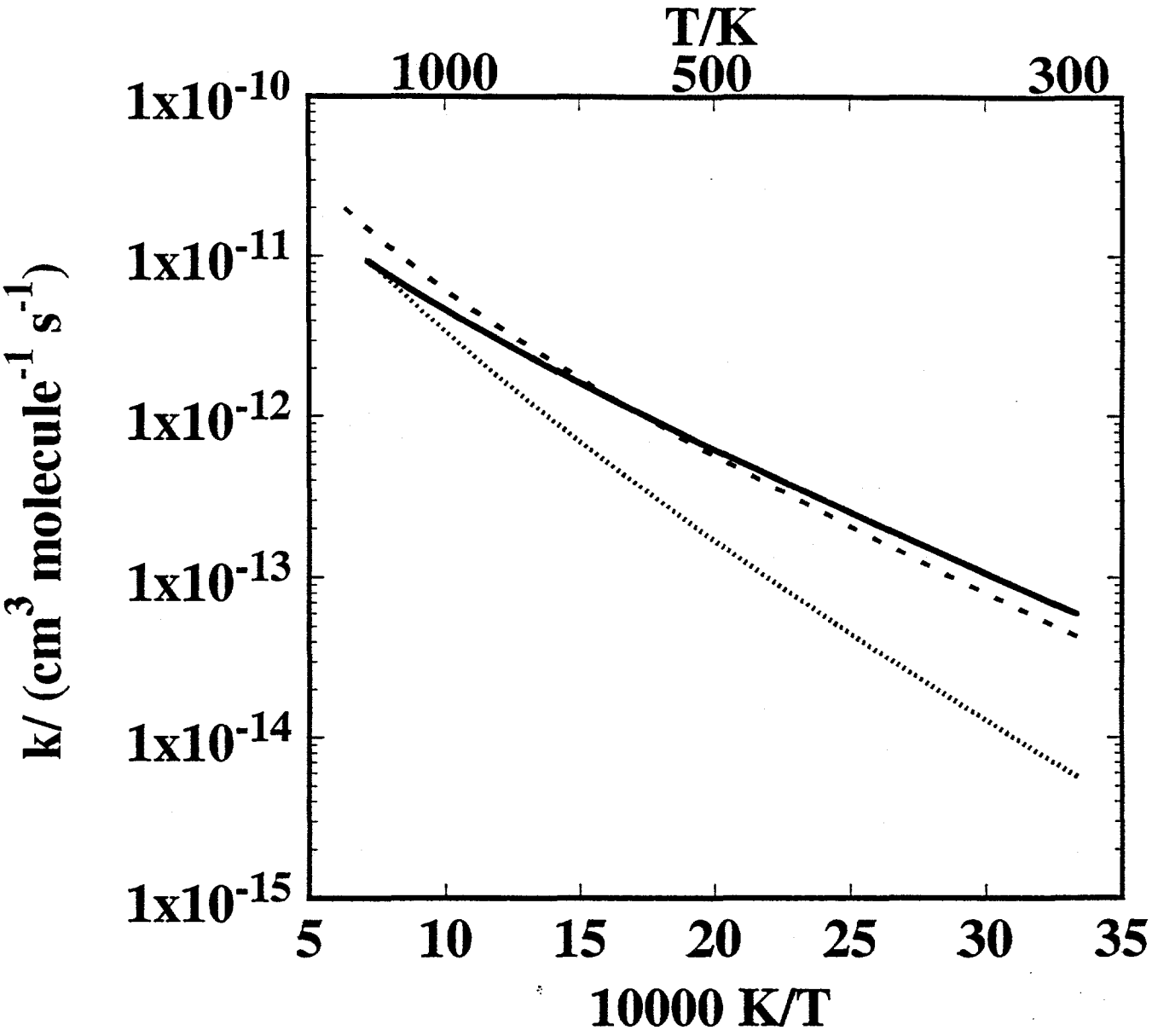
T/K
1000
500
300
1x10-10
1x10-11
1x10-12
1x10-13
1x10-14
1x10-15
k/ (cm3 molecule-1 s-1)
5
10
15
20
25
30
35
10000 K/T

FIGURE 4

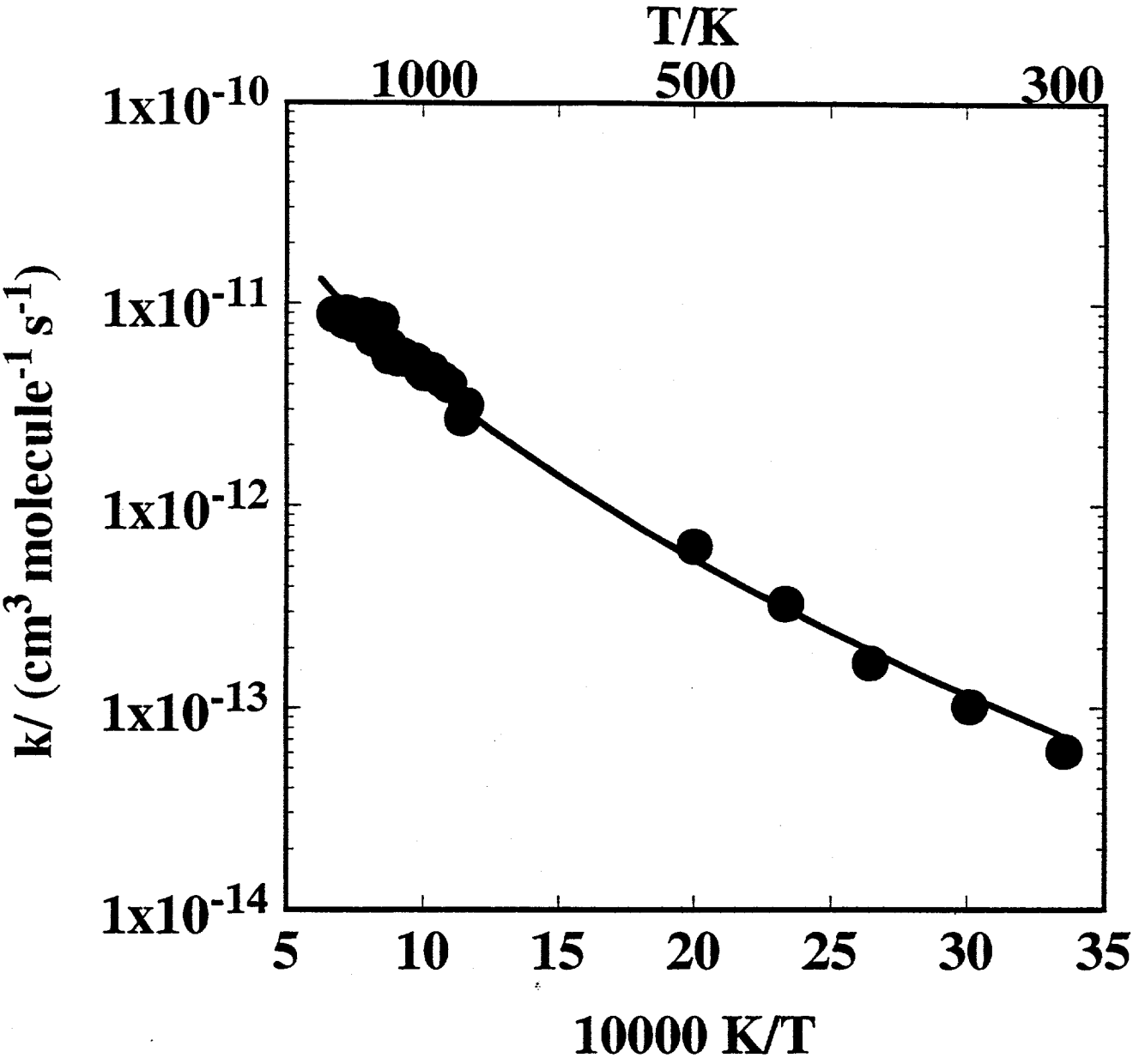
T/K
1000
500
300
1x10-10
1x10-11
1x10-12
1x10-13
1x10-14
k/ (cm3 molecule-1 s-1)
5
10
15
20
25
30
35
10000 K/T

FIGURE 5